# Deblending using the radiality attribute

*Joseph Jennings and Shuki Ronen*


## ABSTRACT

The non-uniqueness of simultaneous source deblending inversion is a challenge in simultaneous source separation. We propose to add another constraint to this inversion using radiality, an attribute that can be computed from multicomponent data that are commonly recorded during ocean-bottom node (OBN) or multi-sensor streamer surveys. We describe a simple, proof-of-concept scheme that demonstrates the use of radiality as an additional constraint and show results on an OBN field dataset.


## INTRODUCTION

Simultaneous source shooting is an emerging method used to reduce acquisition costs while still providing high quality seismic data. Additionally, it is used to improve data quality while keeping the cost constant. In order to accurately image these data, there exist many challenges due to the cross-talk from interfering sources. The process of separating the data and removing the seismic interference between the simultaneous sources is called deblending.

One proposed solution for deblending is to separate the interfering source from the dominant source via a sparse inversion approach (Abma et al., 2010; Ayeni et al., 2011). Intrinsically, this approach poses a highly-underdetermined problem that must be constrained via a regularization term in addition to the data fitting term in the objective function. Effective choices for this regularization have been using continuity in the common-receiver domain.

We propose an additional constraint for deblending inversions from using multi-component data. We show that using additional information from the other components of an ocean-bottom node (OBN) dataset can provide a better starting model for deblending inversion. As of now, we are using four component OBN data. However, this method is applicable to three component multi-sensor streamer data and perhaps also with attributes calculated from single- or dual-component conventional streamer data with the in-line horizontal component computed from the in-line spatial derivative of the data and the cross-line horizontal component unknown.

In Jennings and Ronen (2016), we described both radiality and source similarity attributes. In this report, we further develop the radiality attribute. We first describe how using the radiality attribute can provide additional information that can aid deblending inversions and show examples on a synthetically blended field dataset from the North Sea (Alves, 2015). We then provide a simple proof-of-concept method that shows that using radiality, we can create more accurate starting models for a deblending inversion and we demonstrate these results on the same North Sea dataset.

# METHODOLOGY

## Additional information from multicomponent data

To understand how using multicomponent data can aid in deblending seismic data, let us consider a simple example. Figure 1 shows the acquisition geometry of a synthetically blended dataset from the Forties oil field in the North Sea. Note that because these data were blended synthetically, this creates a worst case scenario in terms of signal to noise ratio.

Figure 1: The simultaneous source acquisition geometry over the Forties oil field in the North Sea. Only two sources were used in the blending of these data and their locations are indicated by the red and blue circles. Both sources circled around a platform under which ocean-bottom nodes were positioned. The black star indicates the location of the receiver node use in this study. [**ER**]

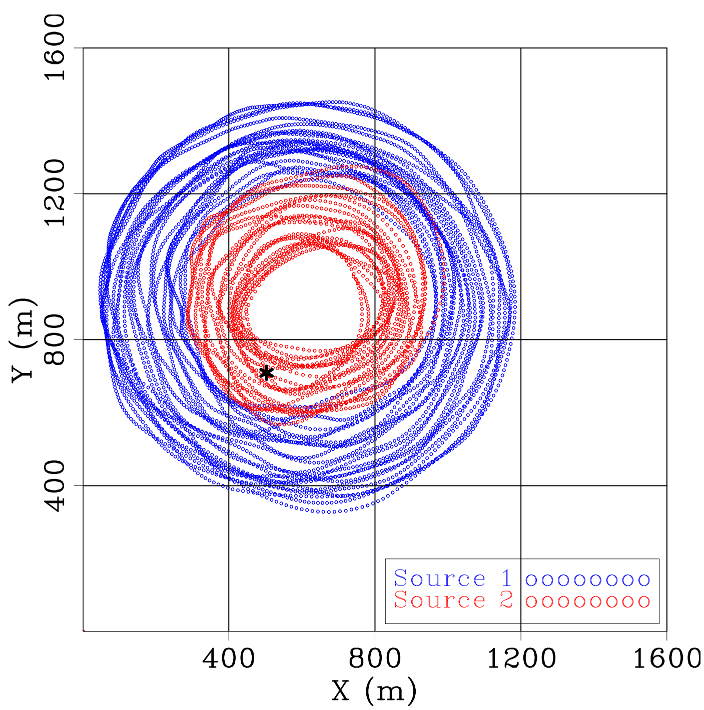


For the purpose of explaining the radiality attribute, let us consider only two shots that have a source-receiver azimuthal difference of approximately 90°. These two source positions and the node location are shown in Figure 2. The corresponding multicomponent data recorded at the node location from these two shots are shown in Figure 3. Examining the hydrophone and vertical components (Figures 3(a) and 3(b)), we can clearly observe both source 2 and source 1 as expected from a trace of the blended common receiver gather. In Figure 3(c), we observe the radial trace rotated toward the azimuth of source 1. It is apparent that after rotation, source 1 is the dominant source on the radial component and source 2 has much less energy. Likewise, on the transverse component (Figure 3(d)), which points almost directly toward the source 2 azimuth, source 2 is the dominant source and source 1 has much less energy. This is because almost all the waves that radiate from any acoustic source have radial polarity.

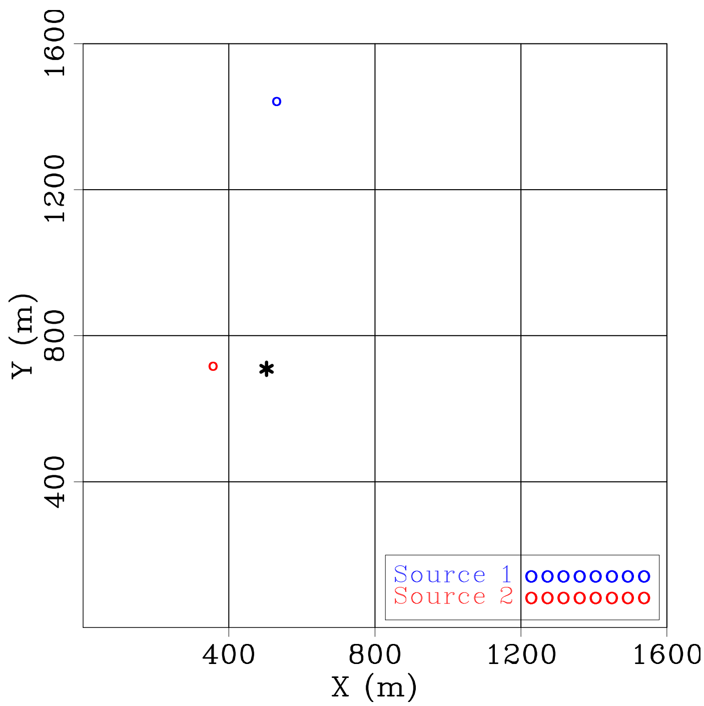


Figure 2: Two source locations selected from the locations shown in Figure 1. These locations were chosen as they have an approximate source-receiver azimuthal difference of 90°. [**ER**]

We observe a similar result when the data are rotated toward the azimuth of source 2. Figure 4 shows the result of rotating the data toward the azimuth of source 2. Again, observing the radial and transverse components (Figures 3(c) and 3(d)), it is clear that by rotating into the azimuth of source 2, we can identify the dominant source at any time on a blended trace.

## Radiality and deblending

To turn this identification capability into a deblending method, we produce a radiality attribute which may be used as a constraint in an inversion problem. Using radiality, we can detect the presence of the dominant source at any time on a blended trace from a multicomponent common receiver gather. This information stems from the fact that when rotating into the different source-receiver azimuths, one source is significantly more radial than the other relative to the location of the node. Therefore, we desire to quantify how radial the data are at any given time. In Jennings and Ronen (2016), we defined the radiality of a trace as the ratio of the radial and transverse envelopes. Thus, the radiality is small when non-radial interfering sources are recorded. As an extension of radiality, we define a new attribute as the ratio of the transverse envelope and the radiality. Mathematically, this may be written as:

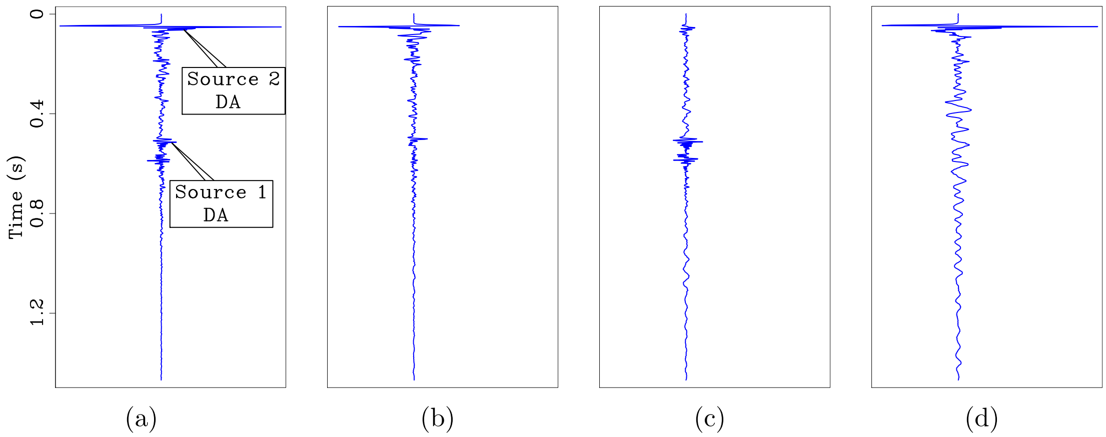


Figure 3: Data recorded from source locations shown in Figure 2. 'DA' indicates direct arrival. Source two was recorded first and then source one. Also note that source two is much stronger than source one in amplitude due to its proximity to the node. Panel (a) shows the hydrophone component, (b) the vertical component, (c) the radial component rotated toward the azimuth of source 1, and (d) the transverse component (rotated perpendicular to the azimuth of source 1). Note how source 1 is distinct in (c) and source 2 in (d). [**ER**]
joseph1/. b12-h-raw877-anno, b12-v-raw877, b12-r-raw877, b12-t-raw877

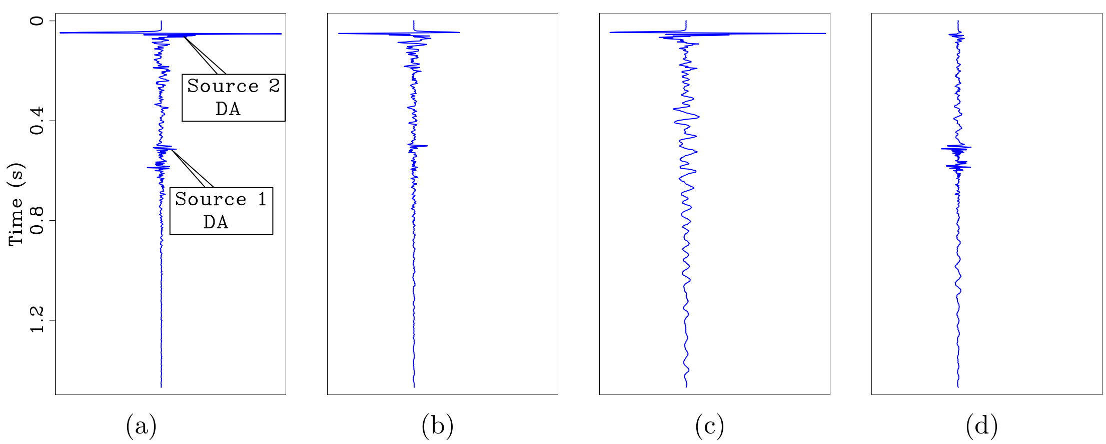


Figure 4: Same as data shown in Figure 3 but now rotated into the azimuth of source 2. As in Figure 3, 'DA' indicates the direct arrival. Panel (a) shows the hydrophone component, (b) the vertical component, (c) the radial component rotated toward the azimuth of source 2 and (d) the transverse component (rotated perpendicular to the azimuth of source 2) Note how source 2 is distinct in (c) and source 1 in (d). [**ER**]
joseph1/. b21-h-raw624-anno, b21-v-raw624, b21-r-raw624, b21-t-raw624

$$\frac{E_{\text{transverse}}}{\text{Radiality}} = \frac{E_{\text{transverse}}}{\frac{E_{\text{radial}}}{E_{\text{transverse}}}} = \frac{E^2_{\text{transverse}}}{E_{\text{radial}}},$$

which is just the ratio of the square of the transverse envelope and the radial envelope. We denote this new radiality attribute as $\frac{T^2}{R}$. Figure 5 shows the overlay of this attribute over the hydrophone component. From this figure, it is clear that the $T^2/R$ attribute detects the interfering source relative to the dominant source. Note that from this point onward when referring to the $T^2/R$ attribute, we use the term "radiality attribute".

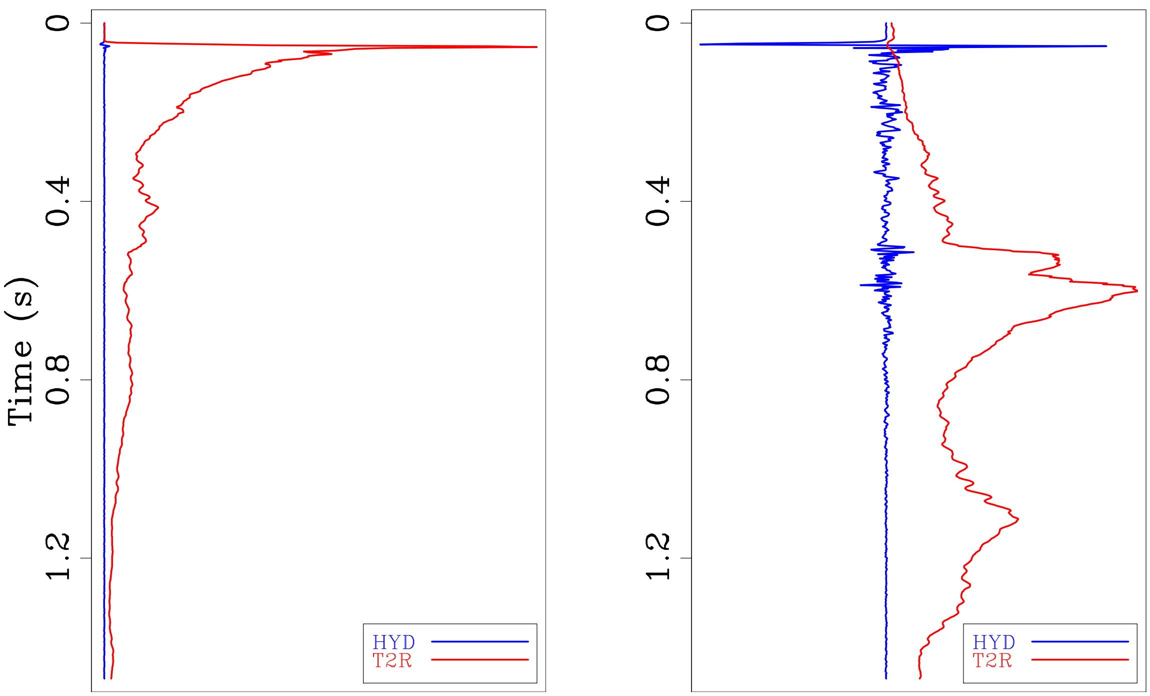


(a) (b)

Figure 5: Radiality attribute overlain on the hydrophone component. The radiality attribute of source 1 is shown in panel (a) and the radiality attribute from source 2 is shown in panel (b). In panel (a) the radiality attribute is maximum over the direct arrival of source 2, the interfering source. Likewise, in panel (b), the radiality attribute is maximum over source 1, the interfering source in this panel. [**ER**]

## RESULTS

As a simple proof-of-concept of how this radiality attribute can be used in a deblending inversion, we use it to mute the data from the interfering source and then interpolate to fill in the gaps. The interpolated data give us a better starting model for a deblending inversion. Figure 6 shows 1000 traces of the blended hydrophone component of a common receiver gather from the same North Sea, Forties oil field dataset described previously. The computed radiality attribute on this common receiver gather is shown in Figure 7(a). The oscillating light and dark regions are indicative of the azimuthal difference of the sources (i.e. brighter regions indicate an azimuthal difference closer to 90°). Figure 7(b) shows the deblended data after muting the interference and linearly interpolating from shot to shot.

Comparing Figures 6 and 7(b) it is clear that in the regions of approximately 15-90°azimuthal difference between the sources, much of the interference was removed. However, in areas where this is not the case, the interference is still largely present. Figures 8(a)-8(c) show a zoom-in of each step of the deblending scheme. Again, from these figures it is clear that the radiality attribute has successfully detected much of the interference in regions of large azimuthal difference. In regions where the azimuthal difference is small, the interference has been largely untouched.

As we only linearly interpolated from trace to trace, in regions where there exist steep events or large gaps, the linear interpolation will not be very accurate. If we first flatten the data with a normal moveout correction (NMO), and interpolate the flattened gathers, we achieve better interpolated data. The results of interpolating in the NMO domain are shown in Figure 8(d). The difference between this result and the original unblended data (shown in Figure 8(e)) is shown in Figure 8(f). In this figure, it is clear that much of the interference has been removed. Note also the errors in interpolation near the direct arrival (between the shot range 200-250 and 500-600).

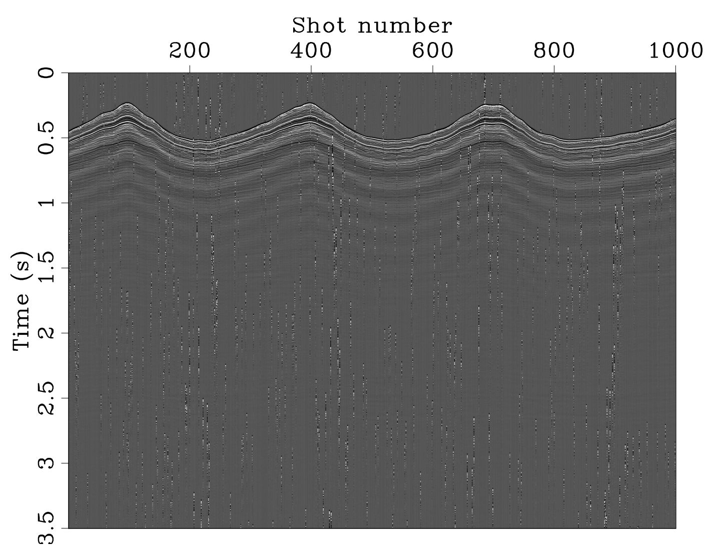


Figure 6: 1000 traces from the hydrophone component of a blended common receiver gather from the Forties oil field data. [**ER**]

## DISCUSSION

One limitation of this method, as shown in Figure 8, is that if the interfering source is in the same azimuth as the primary source, or 180° away, the radiality attribute is of little use. While it is possible to extend the method to 180° separation, it is inherently impossible to extend it to 0° separation. Another limitation, which was not apparent in the deblending demonstration of Figure 8 but is a potential problem,

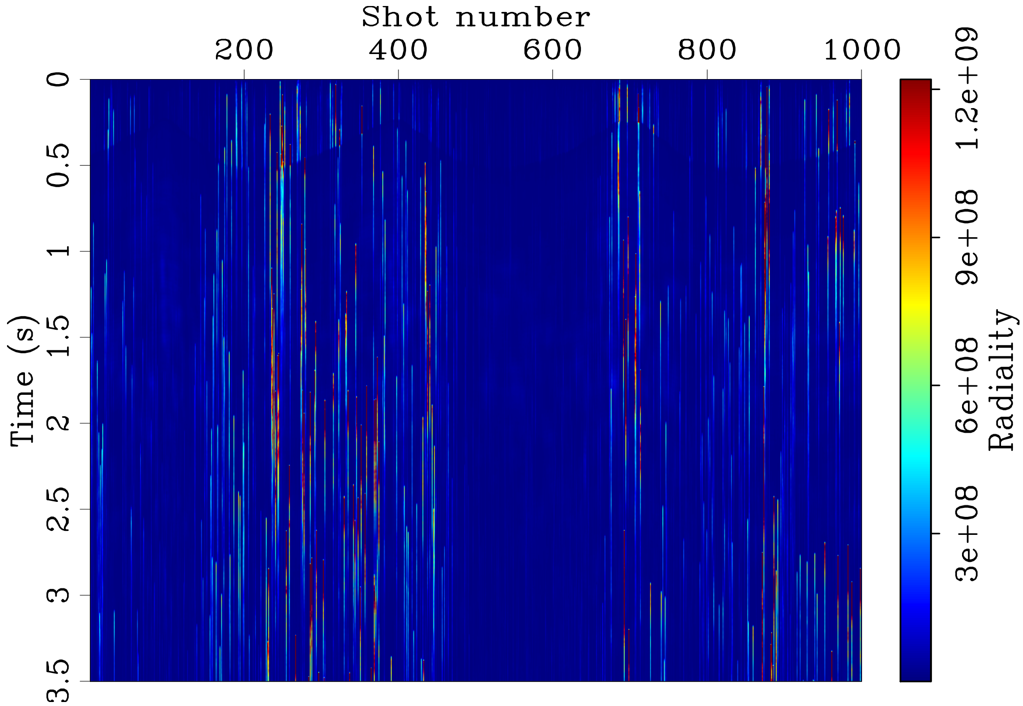


(a)

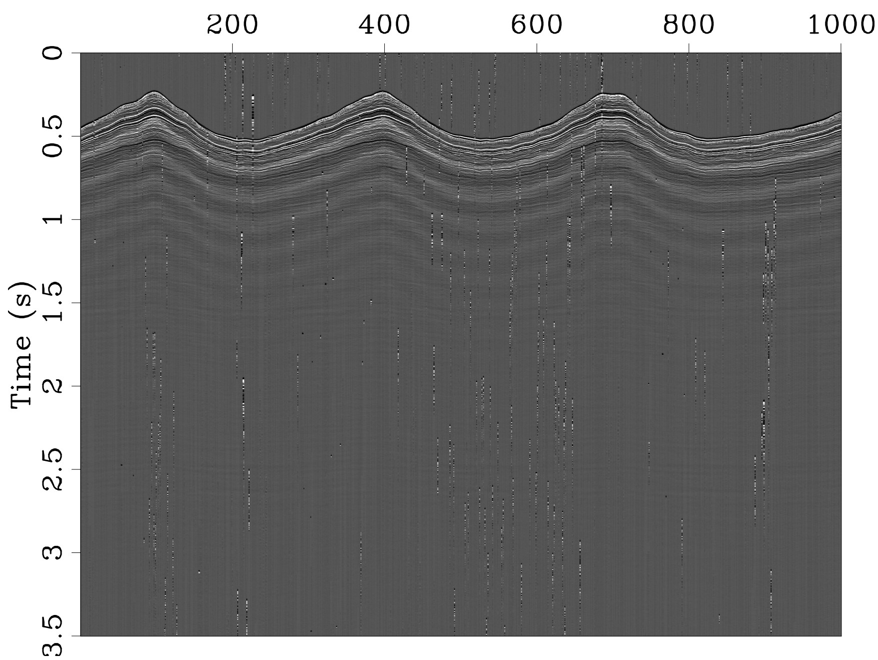


(b)

Figure 7: (a) The radiality attribute computed over the 1000 traces shown in Figure 6. (b) The deblended data obtained via muting the interfering shots and then linearly interpolating from shot to shot. Note in panel (a) that the oscillating dark and light regions occur due to the changing source azimuths. From panel (b) it is clear that where the radiality attribute is high (the regions where the azimuthal difference between the sources is approximately 15-90°), our deblending scheme removes the interfering sources with much greater success. [**ER**] joseph1/. t2or-002b12, interped-002b12

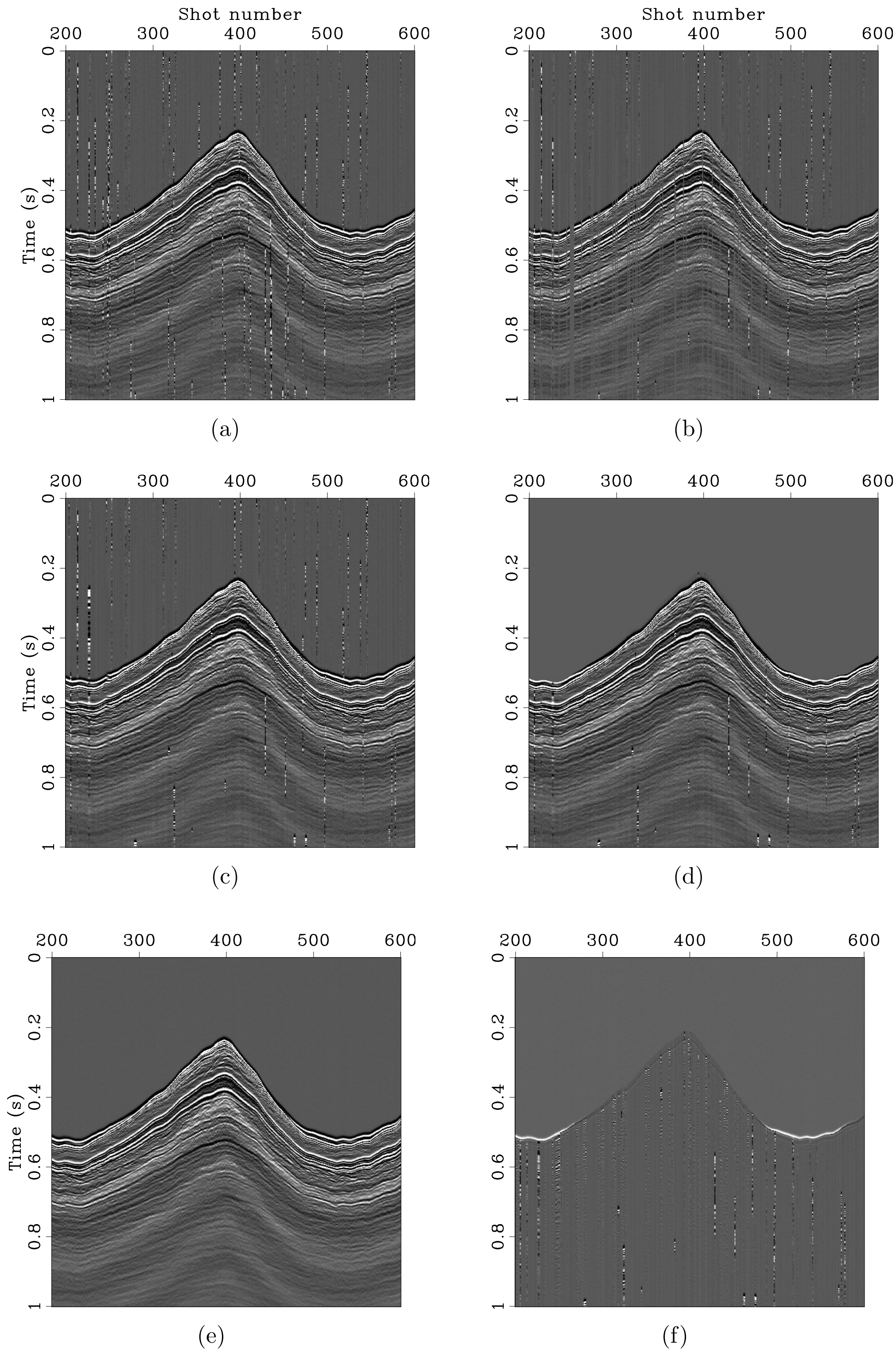


Figure 8: A zoom-in of the common receiver gather from shot 200 to 600. (a) The synthetically blended data. (b) The data after muting the interfering shots using the radiality attribute (Figure 7(a)). (c) The muted data linearly interpolated from shot to shot. (d) The muted data linearly interpolated from shot to shot in the NMO domain. (e) The original unblended data included for comparison and (f) the difference between the deblended data shown in (d) and the unblended data (e). [**ER**]

is related to the synchronization of the sources. If the sources are synchronized, then filling in the declared missing data with interpolation will be impossible as the gaps will extend laterally from one trace to another on a common receiver gather. Both of these limitations can be mitigated by survey design to minimize the shots with small azimuthal difference and to avoid synchronization between the sources. For example, avoiding synchronization could be done if each source vessel moved at a slightly different velocity. Mitigated or not, with these limitations, radiality provides additional information and serves as an additional constraint for deblending inversions.

Another limitation of the method is that primary source waves may arrive on a non-radial direction if they are reflected or scattered from the side. Using radiality, such waves may erroneously be identified as seismic interference. For this reason, in the future it will be important to develop a more sophisticated constraint on the seismic interference using a probability instead of a harsh mute as we have shown so far.

## CONCLUSION

We have shown that using radiality, an attribute computed from the horizontal components of the geophone or ocean-bottom node, we can identify the presence of the dominant source at anytime given that the source vessels have different source-receiver azimuths. We provided a simple proof-of-concept example in which using the radiality attribute, we zeroed the energy from the interfering source. We then interpolated the zeroed data which provided a result that has less interference than the blended data and thus could prove to be a more accurate starting model as input to a full deblending inversion.

## ACKNOWLEDGEMENTS

The authors would like to thank Apache Corporation for the permission to show the data and acknowledge the sponsors of the SEP for their financial and intellectual support.

## REFERENCES

Abma, R., T. Manning, M. Tanis, J. Yu, and M. Foster, 2010, High quality separation of simultaneous sources by sparse inversion: Presented at the 72nd EAGE Conference and Exhibition incorporating SPE EUROPEC 2010.

Alves, G., 2015, Overview of the apache forties data set: SEP-Report, **160**, 175–180.

Ayeni, G., A. Almomin, D. Nichols, et al., 2011, On the separation of simultaneous-source data by inversion: Presented at the 2011 SEG Annual Meeting.

Jennings, J. and S. Ronen, 2016, Separation of simultaneous source blended data using radiality and source similarity attributes: SEP-Report, **163**, 239–256.